Jurnal Mekanikal
December 2008, No. 26, 37 - 48

EFFECT OF SURFACE ROUGHNESS ON DRAG OF LOGGERHEAD CARAPACE

Alan Chan Kah Poh[1], Cheng See Yuan[1*], Ahmad Kamal Mat Yamin[1], Ainil Jesita Jalaluddin[1], Iskandar Shah Ishak[2], Shuhaimi Mansor[2]

[1]Faculty of Mechanical Engineering,
Universiti Teknikal Malaysia Melaka,
Hang Tuah Jaya,
75450 Ayer Keroh, Melaka

[2]Faculty of Mechanical Engineering,
Universiti Teknologi Malaysia,
81310 UTM Skudai, Johor

ABSTRACT

The present investigation primarily studies the effect of surface roughness on the drag coefficient, Cd of a Loggerhead sea turtle carapace using a subsonic wind tunnel. The pressure coefficient, Cp distribution across the Loggerhead carapace was also investigated and is compared to the Cp trend of an airfoil in order to deduce the aerodynamics features of the Loggerhead carapace. One-to-five-scaled models are created based on the dimensions of a real Loggerhead turtle with simplification. Four roughness scales were employed to capture the Cd trend at increasing Reynolds numbers, Re. As expected, the Cd levelled off with Re for all four models investigated. However, the Re where constant Cd began varies with relative roughness of the carapace models. Good correlation between the Cd and relative roughness is obtained. In addition, the wind tunnel results are able to capture the Cp trend of the carapace models and compared to Cp values of an airfoil. Results reveal that the upper surface of the Loggerhead carapace is streamlined but with restrictions of angle of attack.

Keywords: *Drag, roughness, carapace, wind tunnel*

1.0 INTRODUCTION

In the shores of Shark Bay, Western Australia, a relatively undisturbed foraging ground, forms an excellent feeding ground for sea turtles and hosts a rich marine ecosystem [1]. A research led by Mike Heithaus over a span of ten years has revealed the fact that green sea turtles (Chelonia mydas) are less likely to be attacked by tiger sharks (Galeocerdo cuvier) when compared to Loggerheads (Caretta caretta), sometimes as much as five times [2]. Although both are of the

* Corresponding author: Email: cheng@utem.edu.my

same family of Cheloniidae, the green and Loggerhead sea turtle are as different as tanks and flying saucers.

The cause to why Loggerhead sea turtles are at higher risks of being attacked by tiger sharks at Shark Bay, Western Australia are comprised of many factors, one of which is the Loggerhead's habit of not cleaning its shell thus allowing the build-up of roughness over time. However, to the author's knowledge, there has yet to be any comprehensive study on how drag upon the shell is influenced by the roughness build-up on loggerhead carapace. In the context of this project, the main objective is to study the effects of roughness built up on the shell of loggerhead sea turtles in relation to drag.

The investigation had focused on the Loggerhead sea turtle that dwells within the Caribbean Seas near Curacao, Netherlands Antilles. A simplified model was created based on the dimensions of the real Loggerhead sea turtle. Verification of the designed model was reflected based on the values of blockage ratio. Following this, the surface roughness of the models was defined and analysis based on wind tunnel testing results was done to examine static drag in relationship with the surface roughness.

2.0 WIND TUNNEL MODEL

2.1 Model Dimensions

The 1:5 scaled, simplified wind tunnel models of the loggerhead turtle carapace were created based on the actual turtle carapace dimensions as presented in the study by Epperly et al., and the dimensioning conventions used by Wyneken [3]. Accordingly, the Standard Carapace Length (SCL) and Standard Carapace Width (SCW) of 0.92 m and 0.63 m, respectively, were adopted as the length to width ratio of the scaled down carapace models of the present study.

This model scale has also taken into consideration the blockage ratio and dynamics similarity of wind tunnel test, which entails information of the actual swimming speed of the loggerhead turtle. Hence, the mean swimming speed of 0.5721 m/s presented by Nagelkerken et al. [4] is adopted. As for the temperature and density of the sea water, the values are taken at 26.7 ºC and 1027 kg/m^3, respectively. The design of the model is first created using a commercial CAD program, SOLIDWORKS 2006, as shown in Figure 1. It is then fabricated using thermoplastic via Rapid Prototyping with the final model as shown in Figure 2.

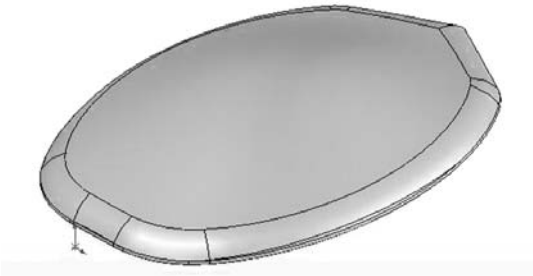

Figure 1: Simplified wind tunnel model of loggerhead carapace

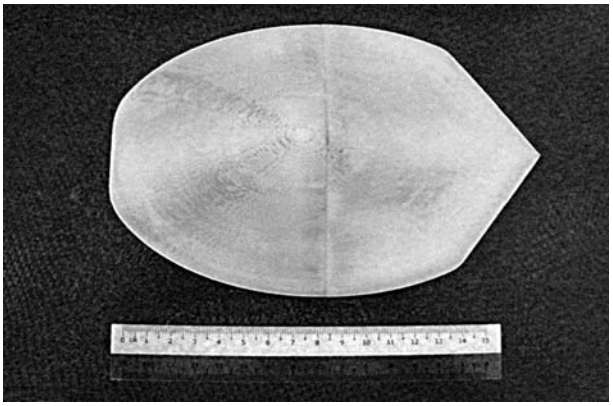

Figure 2: Model product of rapid prototyping

The blockage ratio of less than 0.05% based on the requirement of aeronautics study is attained. The frontal area used for the calculation of blockage ratio is estimated using method introduced by Scott Thor [5].

2.2 Surface Roughness Definition

In the present study, the relative roughness of a finished surface is defined as follow:

$$\text{Relative roughness} = \frac{\varepsilon}{L} \tag{1}$$

Where ε refers to the mean roughness height of fifteen tabulated points determined with a scope, and L is the chord length of the model. Data was retrieved from a test-slate with the respective roughness to be tabulated. In total, four roughness models were used as summarized in shown in Table 1. For convenience in the discussion, the models are designated as Models A, B, C and D respectively.

Table 1: Relative roughness data

Specimen	Relative Roughness
A	Smooth
B	0.430
C	0.456
D	0.556

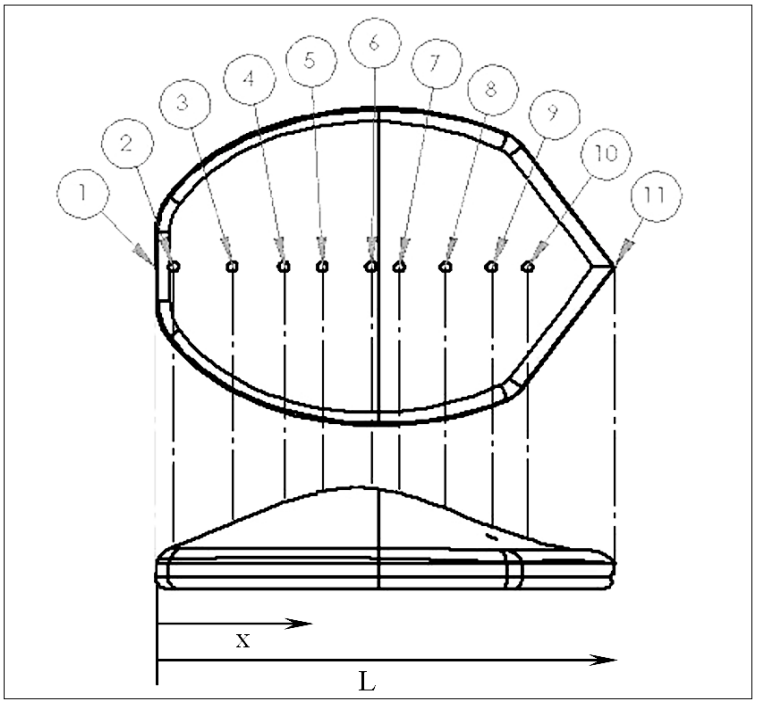

Figure 3: Pressure-tapping numbering

A model with eleven pressure tappings was created as shown in Figure 3, using eleven polyurethane tubes. The relative distance, x/L of the tapping points from the anterior tip is shown in Table 2.

Table 2: Relative distance of tapping points

Tapping no.	Relative Distance from anterior tip, x/L
1	0.00
2	0.04
3	0.17
4	0.28
5	0.36
6	0.47
7	0.53
8	0.63
9	0.73
10	0.81
11	1.00

3.0 WIND TUNNEL TESTING

Aerodynamic static load testing were done on models A, B, C and D to initially obtain the drag coefficient (Cd) values at increasing Reynolds number (Re) ranging from 1.1 x 10^5 to 6.3 x 10^5, in a subsonic wind tunnel with a test section area of 2.0 m (width) x 1.5 m (height). This was followed by the testing of models A and D with multiple angle of attacks ranging from -30 º to +30 º in relative to the horizontal axis, at a fixed Re of 4.5 x 10^5 where positive angular displacement is denoted by clockwise rotation from the horizontal axis as shown in Figure 4.

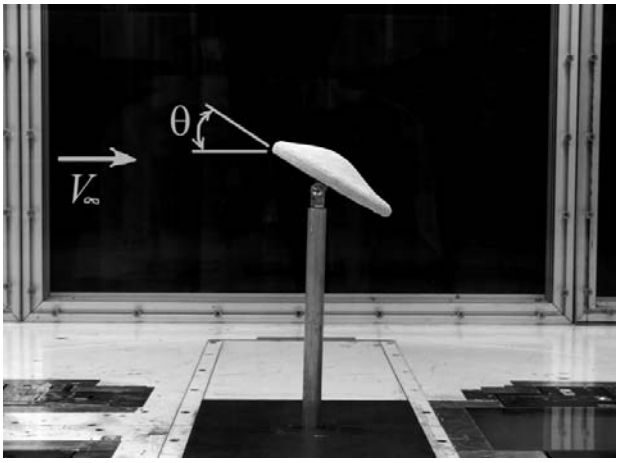

Figure 4: Orientation of angle of attack

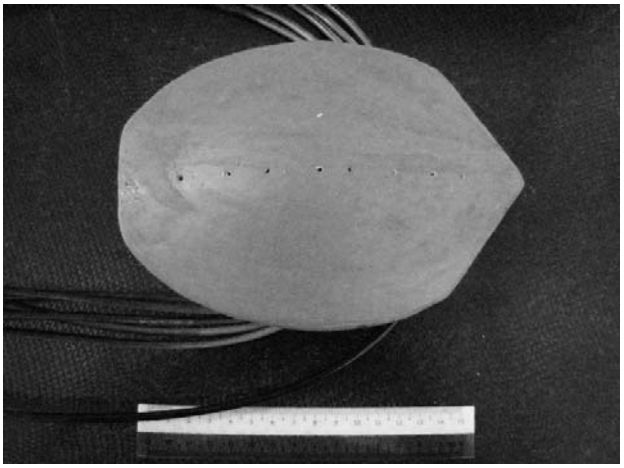

Figure 5: Pressure-tapped loggerhead model

Pressure measurement testing was carried out on the pressure-tapped-model shown in Figure 5. Testing was done at Re ranging from 1.1 x 10^5 to 4.5 x 10^5.

This was followed by subjecting the model to a fixed Re of 4.5 x 10^5 at different angles of attack starting at -30 º to +30 º inclining from the horizontal axis.

A Pitot static tube was also installed at the test section, in order to obtain the free stream static and dynamic pressures. The pressure coefficient (Cp) was determined by the following equation:

$$Cp_i = \frac{P_i - P_\infty}{q_\infty} \tag{2}$$

Where,

i = Taping point number
P_i = Pressure tap at 'i'
P_∞ = Free stream static pressure (Pa)
q_∞ = Free stream dynamic pressure (Pa)

4.0 RESULTS AND DISCUSSION

4.1 Effects of Reynolds Number (Re) on Drag Coefficient (Cd)

Figure 6 shows that Model A registers a high Cd value when Re is 1.1 x 10^5 but the subsequent Cd values show a quick decrement before gradually showing more constant results at the Re approaches the 5.0 x 10^5 region. Model B also starts off at a higher Cd value before having the Cd value decrease as Re increases. Again, the Cd values show little variation as the Re increases past the 5.0 x 10^5 region. Models C and D show similar trends as the earlier two specimens and only differ in terms of the magnitudes.

It was clearly observed that the ending Cd values of Models D, C, B and A are in descending order when the Re is 6.3 x 10^5. The immediate inference that can be made is that a rougher model yields a higher drag coefficient which is a commonly accepted logic in aerodynamic study. More importantly, it also revealed that the critical wind speed in which the drag forces seem to stabilize when Re approaches 4.5 x 10^5. This can be seen from the lack of fluctuation of drag coefficient values as shown in Figure 6.

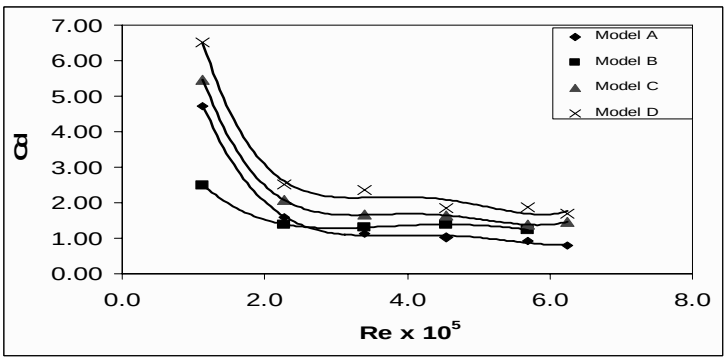

Figure 6: Graph of Cd against Re for different specimens

At Re of 4.5 x 10^5, the values of Cd of Models A, B, C and D are 1.02, 1.39, 1.64 and 1.85, respectively. Comparing this to the Cd values of 0.04, 0.3 and 1.05 for the typical design of an automobile, streamlined body and cube respectively, it is apparent that high Cd values were incurred despite obtaining a repeating and satisfactory trend among the Models [6]. It could be possible that this is the result of systematic error. This is because an internal balance for the load cell was improvised to be attached externally to the Loggerhead model. Thus, the balance support itself would be subjected to the oncoming wind and induce a certain amount of drag, especially against such a somewhat small-scaled model. The amount of the error could be quantified; however, this entails further investigation on the load cell.

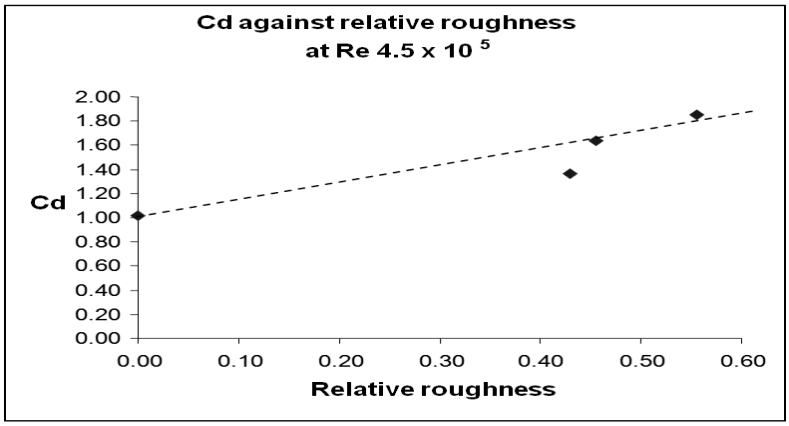

Figure 7: Cd plotted against relative roughness at Re of 4.5 x 10^5

Figure 7 depicts the general relationship that increase in roughness leads to increased friction drag which ultimately induces a higher drag coefficient. A linear relationship may be drawn if assuming that the point that falls outside of the doted line is subjected to random error, which may likely occur if considering the difficulties involve in the measurement of the surface roughness of a profiled surface as described in section 2.2. Perhaps, further study with more measurement points may discern the relationship between drag coefficient and relative roughness more assertively.

4.2 Drag Coefficient (Cd) at Multiple Angles of Attack

Figure 8 depicts the Cd values for Models A and D at multiple angles of attack whereby the positive displacement of the angles is defined as clockwise from the horizontal x-axis. Both models show similar trends in correspondence with the varying angles of attack and ultimately yielding a 'U' trend. This translates that the drag coefficient of the Loggerhead model, regardless of roughness, is maximum when the angle of attack is -30 º. As the angle of attack is decreased to -10 º and 0 º, the corresponding drag coefficients are also decreased. Once the

angle of attack increases from 0 º to 10 º and 30 º ultimately, the drag coefficients increase as well.

Maximum drag occurs at -30 º for both models. It may be due to the fact that at an inclination of -30 º, the entire upper surface profile of the model is directly subjected to the oncoming wind-flow, inducing the air-flow to be directed along the upper surface until the tip while generating a wake region adjacent to the bottom surface. Thus, a substantial pressure drag is created. This compared to when the model is at 30 º, a smaller wake region area adjacent to the upper surface of the posterior half is generated. This may be because air-flow is directed to distribute across the streamline upper surface. The phenomena of negative inclinations having a higher Cd value holds for -10 º and +10 º as well.

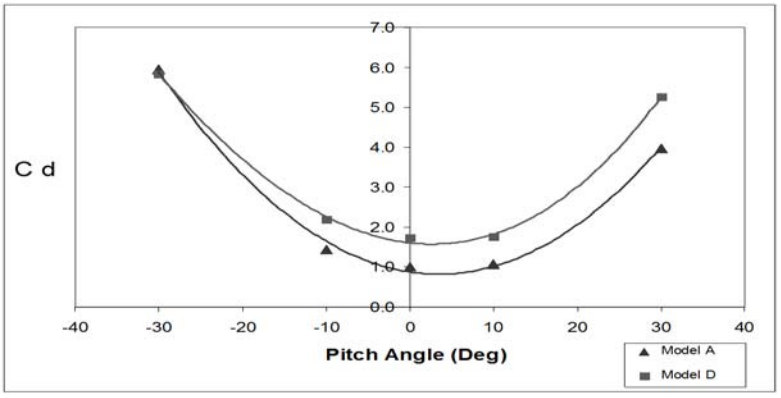

Figure 8: Cd characteristic at different angles of attack at Re 4.5 x 10^5

4.3 Effects of Reynolds Number (Re) on Pressure Coefficient (Cp)

Tapping 1 yields the highest pressure coefficient. The general trend of the curves show the pressure coefficient decreases steeply from tapping 1 to 2 before slightly increasing at tapping 3. Tappings 4, 5 and 6 gradually decrease whereby tapping 6 is the point whereby least pressure acts upon the Specimen. Upon closer inspection, this statement only holds for all wind speeds except at Re 1.1 x 10^5 whereby the Cp is similar from tapping 5 to 8 due to the fact that the Specimen is subjected to a very low wind speed and Reynolds number. For other cases, a gradual rise in Cp is evident starting at tapping 7 all the way to 11.

One interesting observation is the fact that at tapping 2, the Cp values are generally lower than that of tapping 3 except for the run set at a wind speed of 1.1 x 10^5. This is due to the nature of the geometric position of tapping 2 in the pressure model. A closer look at the model would show that tapping 2 is positioned at a distance very close to the sharp curving corner of the anterior side of the Loggerhead model. As wind currents flow across the model from tapping 1 to tapping 2, much of the current would be directed outwards away from tapping 2 due to the curving corner, creating wakes and a sudden rise in pressure at tapping 3.

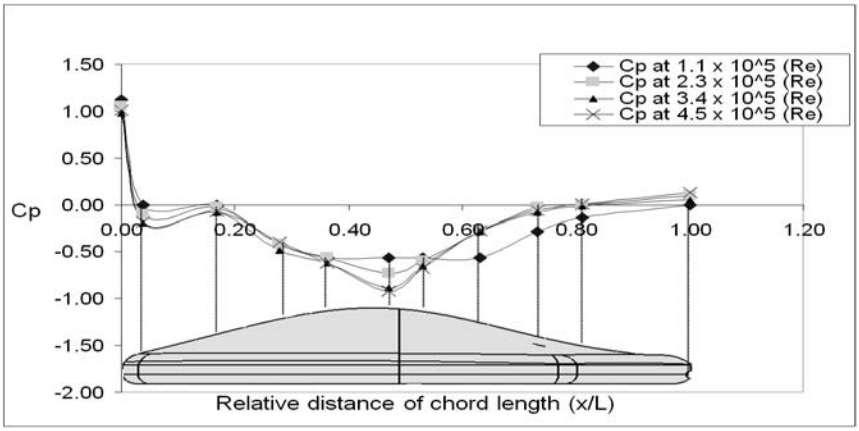

Figure 9: Pressure coefficient Cp distribution at various Re

From this point onwards, the current flow regains energy across the pressure model, and the pressure falls gradually before reaching a minimum value at tapping 6. This is due to the gradual inclination of the model profile that peaks at tapping 6. Again, tapping 7 onwards will show growth in pressure, though still of negative values as the inclination of the profile is reversed before finally reaching a positive value at the posterior end of the model at tapping 11. The negative values of Cp from tapping 2 to 9 reflect and that the profile of the model induces a smoother or faster flow of the wind current thus generating a low pressure region.

Figure 10 depicts the curve trend for the upper surface of an airfoil, shown in Figure 11, at Re of 1.43 x 10^5 and angle of attack of 0º [7]. The curve begins with a positive Cp followed by a steep drop into the negative Cp region and maintains until the very tip of the airfoil. Such a trend is typical of an airfoil as the upper surface of an airfoil is subjected to faster air-flow due to the surface profiling thus creating a low pressure region, as opposed to the bottom surface of the airfoil whereby there is a higher pressure presence, which ultimately generates lift.

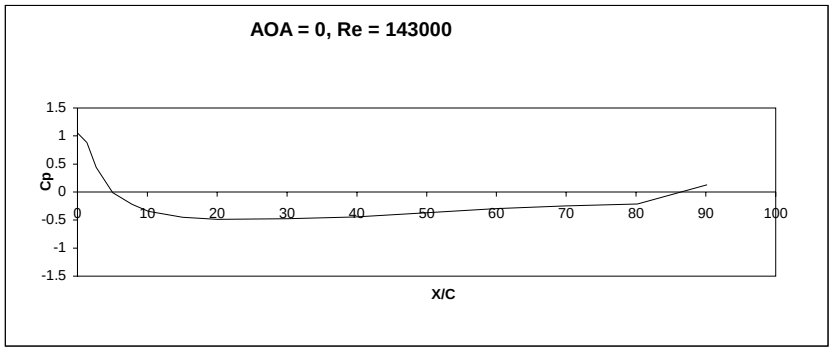

Figure 10: Cd value of airfoil against relative distance of chord length [7]

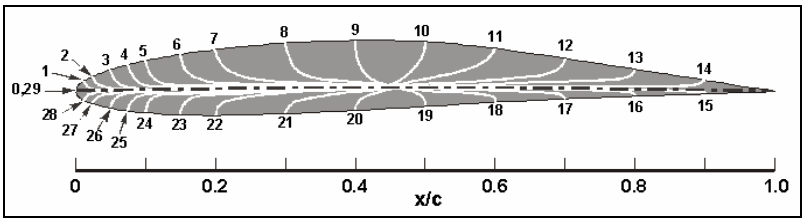

Figure 11: Airfoil tapping scheme [7]

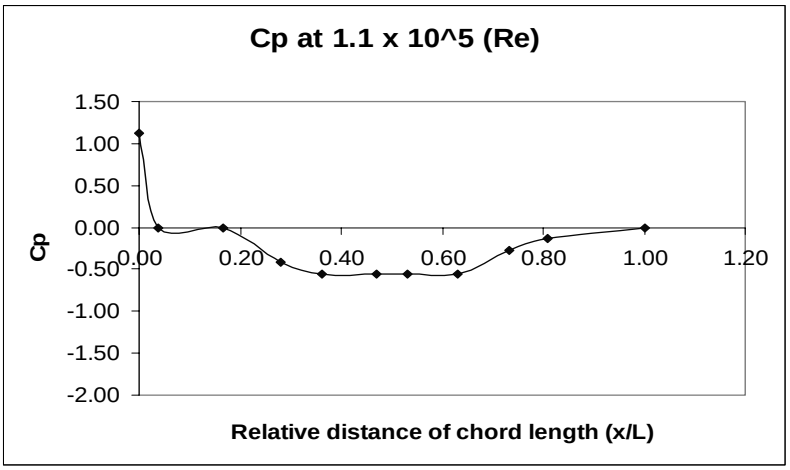

Figure 12: Cp against relative distance

Figure 12 shows the curve trend for the Loggerhead model at Re of 1.1x 10^5 and angle of attack of 0º. Overall, the curve signifies a similar trend to that of the airfoil's whereby the initial high Cp value drops drastically to a negative Cp value and this negative pressure zone maintains until the tip. However, there is a rise is pressure after point 2 due to the geometric profile of the anterior edge of the model that has a flattened face. This could result in a disruption of the air-flow and thus a gain in pressure at point 3. The comparison between the two curves suggests that the upper surface of the Loggerhead model is streamlined as that of the airfoil's surface.

4.4 Pressure Coefficient (Cp) at Different Angles of Attack

Figure 13 represent the plotted data of pressure coefficient at different pitch or angles of attack. At an angle of -10º, it can seen the highest pressure is at point 1, gradually decreasing to point 6 before increasing once more to a pressure coefficient bordering about the value of 0.1.

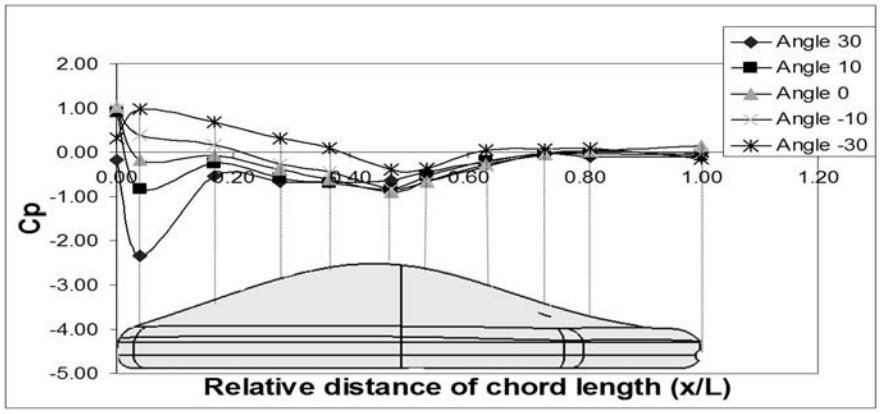

Figure 13: Cp at various angles of attack against relative distance of chord length

Despite also being a negative-valued angle of attack, at -30º, the curve trend is very much different to that of -10º. Evidently, the highest pressure has shifted to point 2. This is very much due to the fact that at a steeper angle, point 2 is subjected to a more direct contact to the oncoming wind current, thus a higher pressure area compared to point 1 which is located at the lateral edge of the anterior part of the Loggerhead model.

At an angle of 10º, it is clearly that the trend mimics that of 0º discussed earlier. However, at this inclined angle, the initial pressure drop is greater just as the latter pressure rise is steeper when compared to the trend of the Specimen at 0º. This signifies that the anterior portion of the model is subjected to a faster flowing current distribution acting over the surface and slows down considerable as it approaches the posterior half of the model. At an angle of 30º, the pressure coefficient is lowest at tapping 2. Not only is more of the flat underside of the model is exposed to the oncoming wind current, much more blockage of the current occurs. This would explain why there is very little variation among the distribution of points albeit showing a fairly recognizable pattern due to nature of the profile of the model. It should be emphasized that tapping 2 experiences such a vast drop in pressure is due to the massive air flow acceleration right around the leading edge of the anterior half of the Specimen, subsequently leading to a low static pressure region.

Overall, this result reflects that the Loggerhead model loses its streamline-feature with the positive increase in the angle of attack.

5.0 CONCLUSIONS

From the tabulated data, it qualitatively shows that the increased surface roughness results in a direct increase in drag regardless of the angle of attack. Furthermore, pressure coefficient comparisons with an airfoil body both quantitatively and qualitatively classify the upper surface of a Loggerhead carapace to be of stream-line-nature so long as its angle of attack is kept to a zero or negative-value (counter-clockwise direction) region from the horizontal axis.

This strongly hints of a new avenue for marine engineering design enthusiasts to venture in as have been spearheaded by a Japanese team led by Konno, A. who have developed a submergence vehicle based on the design of a turtle [8].

ACKNOWLEDGEMENTS

The work reported in this paper has been fully funded by Technical University of Malaysia, Melaka (UTeM).

REFERENCES

1. Heithaus, M.R., Frid, A., Wirsing, A., Bejder, L., and Dill**,** L.M., 2005. The biology of green and loggerhead turtles under risk from tiger sharks at a foraging ground, *Marine Ecology Progress, Series 288,* 285-294.
2. Heithaus, M.R., Frid, A. and Dill, L.M., 2002. Shark-inflicted injury frequencies, escape ability, and habitat use of green and loggerhead turtles, *Marine Biology, 140,* 229-236.
3. Wyneken, J., 2001. The Anatomy of Sea Turtles. U.S. Department of Commerce NOAA Technical Memorandum NMFS-SEFSC-470.
4. Nagelkerken, Pors, L.P.J.J., Hoetjes, P., 2003. Swimming behavior and dispersal patterns of headstarted loggerhead turtles *Caretta caretta*. *Aquatic Ecology*, 37: 183-190.
5. Scott Thor, RGB colour model, (n.d.). Retrieved 20th September 2007, from *http://en.wikipedia.org/wiki/RGB.*
6. Cengel, Y.A. and Cimbala, J.M., 2006. *Fluid mechanics: Fundamental and applications*, International edition, McGraw-Hill, Singapore.
7. Stern, F., Muste, M., Houser, D., Wilson, M., Ghosh, S., 2004. Measurement of Pressure Distribution and Forces Acting on an Airfoil. Mechanics of Fluids and Transfer Processes: Laboratory Experiment #3.
8. Konno, A., Furuya, T., Mizuno, A., Hishinuma, K., Hirata, K. and Kawada, M., 2005. Development of turtle-like submergence vehicle. *Proceedings of the 7th International Symposium on Marine Engineering.*